Formulation of a two-scale transport scheme for the turbulent mix induced by Rayleigh-Taylor and Richtmyer-Meshkov instabilities

Ye Zhou, George B. Zimmerman, and Eugene W. Burke
Lawrence Livermore National Laboratory, University of California, Livermore, California 94551
(Received 30 April 2001; revised manuscript received 26 November 2001; published 3 May 2002)

We develop a two-scale transport model for the turbulent mix induced by Rayleigh-Taylor and Richtmyer-Meshkov instabilities. We generalize the buoyancy-drag model by adding an energy equation for a more complete description of the generated interpenetration between heavy and light fluids. The generalized buoyancy-drag model, in turn, provides an appropriate source to the two-equation turbulence model, which is most suited for the induced turbulent flows. The two-scale transport model has been validated and several illustrative examples will be presented.

DOI: 10.1103/PhysRevE.65.056303 PACS number(s): 47.27.Eq, 47.20.Ma

I. INTRODUCTION

The Rayleigh-Taylor instability (RTI) [1,2] and the Richtmyer-Meshkov instability (RMI) [3,4] play prominent roles in many important scientific and engineering applications. For a supernova event [5], the gravitational pressure from the outer surface of the star leads to the ignition and explosion of the core. This process generates a shock wave toward the outer shells of different densities. The RMI occurs at the perturbed interface separating two fluids of different densities with an impulsive acceleration from the shock wave. For an inertial confinement fusion (ICF) target [6], the dense shell is filled with deuterium-tritium (DT) gas and will be imploded by irradiation methods including laser beams. The RTI occurs whenever a lower density fluid supports a higher density fluid against acceleration. These hydrodynamic instabilities may break up the shell and therefore prevent the ignition of the ICF DT fuel.

Despite the intensive efforts to develop increased computational capabilities, the turbulence transport models remain the most viable approach for the solution of practical astrophysics and ICF problems. The reason for this state of affairs becomes abundantly clear when one considers the difficulties of achieving the required high Reynolds number for the mixing transition to the turbulent mix and of obtaining the desired turnaround time for engineering calculations. These problems, taken together with the fact that the transport models can be incorporated into most ICF or astrophysics computer codes, constitute the major reason for the popularity to pursue this approach.

In this paper, we will formulate a transport model that incorporates advanced features of both the buoyancy-drag and turbulent two-equation models. The framework of the two-scale system provides a description of the interpenetration between the heavy and light fluids along the interface and the production of mostly isotropic turbulent flows, which will be represented by a two-equation turbulence model. The transport model obtained in this study will be shown to yield improved results for both the RTI and RMI induced turbulent flows.

II. EVALUATION OF EXISTING MIX MODELS

Our modeling efforts have been guided by a comprehensive consideration of existing models used for computing the turbulent mix induced by the RTI and RMI. We will review the aspects of various models with an increased order of complexity.

The buoyancy-drag model [7], which computes the evolution of the amplitudes of the mixing region, is the workhorse of many practical mix calculations. Youngs (summarized in the Appendix of Hanson *et al.* [8]), Shvarts *et al.* [9], Dimonte [10], and Cheng, Glimm, and Sharp [11] are examples of published paper describing the buoyancy-drag models. Briefly, the buoyancy-drag model is essentially an equation of motion that balances the inertia, buoyancy, and Newtonian drag forces. The growth of the mixing region depends on the density ratio (therefore, the Atwood number) and the acceleration history. This model is appropriate for the inhomogeneous and anisotropic nature of the interfaces by construction. However, turbulence is not treated directly by the buoyancy-drag model. Furthermore, the buoyancy-drag model should be expanded to incorporate additional physics, such as the adiabatic work (pdV).

We also noted the oversimplification in the traditional two-equation turbulence model [12,13] for the mix calculation. The typical governing equations are the turbulent kinetic energy K and the dissipation rate equation ε. Alternative two-equation models are based on the solution of a modeled transport equation for an integral length scale (the K-L model [14]). The two-equation model can be quite remarkably successful in describing fully developed turbulence, but it may be inherently challenged in dealing with the production of turbulence from the interfacial instabilities. Specifically, we stress [15] that these two-equation turbulence models are isotropic, but the turbulent flows induced by hydrodynamic instabilities are both inhomogeneous and anisotropic.

The multifluid based turbulence model [16], theoretically speaking, could be most complete and accurate. This type of model, however, could also be demanding in both the implementation and numerical computation. Youngs [17,18] developed such a model. In Youngs' approach, turbulence is mod-

eled by a classical version of the two-scale equation [19]. Multifluid based numerical calculations, by their nature, constitute direct computations of the interpenetrations between the heavy and light fluids that require significant computational time in comparison with the single velocity based numerical simulations. It appears that the multifluid model should be subject to further development and validation; a process that brought the single fluid turbulence models to maturity. The significantly increased number of required constants necessary for the multifluid model equations demand careful calibrations against appropriate experimental data or numerical simulations. Also, Youngs' approach does not capture the small amplitude growth phase.

III. FORMULATIONS OF TWO-SCALE TURBULENCE MODEL

We will restrict ourselves to a single velocity framework because of the desire to preserve a relatively quick turnaround time of the ICF calculation and relative ease in implementation in the code structure.

Our transport model, therefore, is an attempt to recover the physics of multifluid based turbulence models, but using a considerably simpler system based on a single velocity framework.

We develop a two-scale model, in spirit of Hanjalić, Launder, and Schiestel [20] and Schiestel [21], to partition the turbulent mix induced by the RTI and RMI into two distinct regions identified as *B* (generalized buoyancy-drag model description) and *T* (turbulence model description), respectively. The two-scale model treats dynamics of interpenetrations between the heavy and light fluids in the *B* region using two equations (a buoyancy-drag model and an energy equation for the buoyancy-drag description). It is widely accepted that the turbulent length and time scales depend strongly on the flow configuration under consideration. Consequently, two-equation models, where transport equations are solved for two independent quantities directly related to the turbulent length and time, represent the minimum accepted level of closure [22] for both *B* and *T* regions. The interfacial region, *B*, also provides the source term to the turbulence region *T*.

We now generalize the buoyancy-drag model by adding an energy equation for a more complete description of the *B* region for the generated interpenetration between the heavy and light fluids.

A. *B* region: Original buoyancy-drag model

The standard buoyancy-drag model [7–11] takes the form

$$\frac{dV_i}{dt}-\beta Ag=-C_D\frac{\rho_i}{\rho_1+\rho_2}V_i|V_i|\frac{1}{h_i}. \tag{1}$$

Here $V_i=dh_i/dt$, where h_i is the amplitude, and $i=b$ corresponds to bubbles and $i=s$ represents spikes. The Atwood number is $A=(\rho_2-\rho_1)/(\rho_2+\rho_1)$ and g is the acceleration, ρ_2 and ρ_1 are the density for heavy and light fluids, respectivel. β depends on h, A, and wavelength λ. $C_D=2.5$ is the drag coefficient.

The amplitudes for the growth of bubbles and spikes, h_i, can be deduced from the definition $V_i=dh_i/dt$. It is then appropriate to make the correspondence between the buoyancy-drag model and the governing equation for the length scale of the generalized buoyancy-drag description region.

B. *B* region: Energy equation for the buoyancy-drag description

Moreover, a new equation for the energy E_B should be developed for the *B* region of interpenetration between the heavy and light fluids in order to incorporate additional physics, such as the pdv work and diffusion transport.

We now show that the governing equation for E_B can be deduced from the standard transport model [12], which was developed to provide the computation of the specific turbulent kinetic energy and to account for some limited nonlocal and historic effects in the determination of the turbulent transport coefficients. The transport equation is written as

$$\rho\frac{DE_B}{Dt}=-P_B\vec{\nabla}_L U+\frac{\partial}{\partial x_i}(\rho\vec{\vec{D}}_B\cdot\vec{\nabla}E_B)+S_B-\rho\varepsilon_B \tag{2}$$

where $D/Dt=\partial/\partial t+\overline{u}_i\partial/\partial x_i$ denotes the substantial derivative. Here L is the direction of normal to the interface and P_B is the pressure along the interface. $S_B=\rho\vec{w}\cdot\vec{U}$ is a source, where $\vec{U}+\vec{w}$ is the volume-weighted velocity. $\varepsilon_B=E_B^{3/2}/L_B$ is the dissipation of energy into the turbulence region *T*. The form of the diffusion tensor $\vec{D}$ will be defined later. The simplification of the standard one-equation model [12] involves omitting the production of kinetic energy resulting from the Reynolds stress.

Now, in the case where we may justifiably limit our attention to a single, dominant length $L_B=\max(h_b,h_s)$,

$$\rho\frac{DE_B}{Dt}=-P_B\vec{\nabla}_L U+\vec{\nabla}\cdot\rho\vec{\vec{D}}_B\cdot\vec{\nabla}E_B+S_B-\rho\frac{E_B^{3/2}}{L_B}, \tag{3}$$

where the loss of energy to turbulence is given [12] by ε_B.

C. The momentum equation

$$\rho\frac{DU}{Dt}=-\nabla(P+Q+P_T)-\nabla_L P_B \tag{4}$$

where P and P_T are the hydro and turbulence pressures, respectively. We introduce Q to denote the artificial viscosity (see, for example, Ref. [23]). The concept of artificial viscosity is introduced into the inviscid Euler equations in order to automatically ''capture'' shock wave discontinuities.

Now within the turbulence region, it is reasonable to assume that the turbulent flow is both homogeneous and isotropic when the Reynolds number is high. As a result, the standard two-equation K-ε model [12] is appropriate for this case, where transport equations are solved for two independent quantities, providing the minimum accepted level of closure [22]. The generalized buoyancy-drag model provides an appropriate source from the interfacial region to the tur-

bulence region. This should compare to the work of Gauthier and Bonnet [13] where only a K-ε model is used to study the turbulent mix.

D. *T* region: The kinetic energy equation

The source of the turbulent kinetic energy K is provided by the energy equation of the generalized buoyancy-drag model $\rho {E_B}^{3/2}/L_B$,

$$\rho \frac{DK}{Dt} = -P_T \vec{\nabla}\cdot\vec{U} + \vec{\nabla}\cdot\rho\vec{\vec{D}}_K\cdot\vec{\nabla}K + \rho\frac{E_B^{3/2}}{L_B} - \rho\varepsilon. \quad (5)$$

The governing equation for the dissipation rate ε is given next. P_T is the pressure from turbulence.

E. *T* region: The dissipation rate equation

$$\rho \frac{D\varepsilon}{Dt} = -\frac{2}{3}\rho\varepsilon\vec{\nabla}\cdot\vec{U} + \vec{\nabla}\cdot\rho\vec{\vec{D}}_\epsilon\cdot\vec{\nabla}\varepsilon + C_{\varepsilon 1}\rho\frac{E_B^{3/2}}{L_B}\frac{\varepsilon}{K} - C_{\varepsilon 2}\rho\frac{\varepsilon^2}{K}. \quad (6)$$

The production of the dissipation rate has a similar format as that of the turbulent kinetic energy equation $\rho E_B^{3/2}/L_B\varepsilon/K$. In Eq. (6), $C_{\varepsilon 1}=1.44$, and $C_{\varepsilon 2}=1.92$.

Apart from the source term, our K-ε model is standard and well documented [12].

F. The internal energy equation

The dissipation of the kinetic energy is converted into the internal energy i, which has the following form:

$$\rho\frac{Di}{Dt} = -(P+Q)\vec{\nabla}\cdot\vec{U} + (P+Q)\vec{\nabla}\cdot\overline{w} + \vec{\nabla}\cdot\rho\vec{\vec{D}}_i\cdot\vec{\nabla}i + \rho\varepsilon, \quad (7)$$

where constant $\sigma_i = 0.9$.

G. The diffusion coefficient

The diffusion term is primarily responsible for the spreading of the mixing zone. A major outcome of the present study is the tensorial form of the diffusion coefficient

$$\vec{\vec{D}}_x = D\hat{L}\hat{L} + D_x\hat{I}\hat{I}, \quad (8)$$

where $\hat{L}$ is the direction normal to the surface, $x = B, K, \epsilon, i$, and the diffusion coefficients are determined from two governing equations of the B and T regions below, respectively. As a result, the two-scale mix model can be applied directly to either two or three dimensions.

The turbulence diffusion coefficient is

$$D_x = \frac{C_\mu}{\sigma_x}\frac{K^2}{\varepsilon}. \quad (9)$$

We have designed the diffusion coefficient within the B region to maintain a linear volume fraction distribution in a symmetrically growing one-dimensional mix region. Multiplying this by a constant less than unity then allows one to obtain the usually desired S shaped curve. The diffusion coefficient is calculated in any geometry solely by solving the diffusion equation given the mix region boundary and its local growth rate normal to the boundary $\dot{h}$.

In general $D(\vec{x})$ is found by solving

$$\nabla^2 D + S = 0, \quad (10)$$

where $D(\vec{x}) = 0$ on mix region boundaries. Here S is is obtained from

$$\nabla^2 S = 0,$$

where $S(\vec{x}) = 2\dot{h}\mathfrak{A}/\mathfrak{B}$ on the boundaries and $\mathfrak{A}/\mathfrak{B}$ is the surface to volume ratio of the mix region.

For the symmetrical one-dimensional case ($-h \leqslant x \leqslant h$),

$$S(-h) = \frac{\dot{h}}{h} \quad \text{and} \quad S(h) = \frac{\dot{h}}{h}, \quad (11)$$

so that

$$S(x) = \frac{\dot{h}}{h} \quad (12)$$

and

$$D(x) = M\frac{\dot{h}}{2h}(h-x)(h+x), \quad (13)$$

with typical value $M = 0.6$. By substitution one shows that this maintains a linear volume fraction distribution $f(x)$ from

$$\dot{f} = \frac{\partial}{\partial x}\left[D(x)\frac{\partial f}{\partial x}\right], \quad (14)$$

where

$$f = \frac{1}{2}\left(1 + \frac{x}{h}\right), \quad (15)$$

$$\dot{f} = -\frac{\dot{h}}{2h^2}x. \quad (16)$$

A referee called to our attention that the diffusion coefficient determined above is essentially the same as that reported by Alon and Shvarts [24]. Cheng, Glimm, and Sharp [25] also presented a derivation of the diffusion coefficient which is similar, but not identical to that derived in this paper and discussed by Alon and Shvarts [24].

H. Standard *K*-ε model constants

All of these constants adopted for our model are also standard and have been used routinely in engineering calculations. The values of these constants were obtained from care-

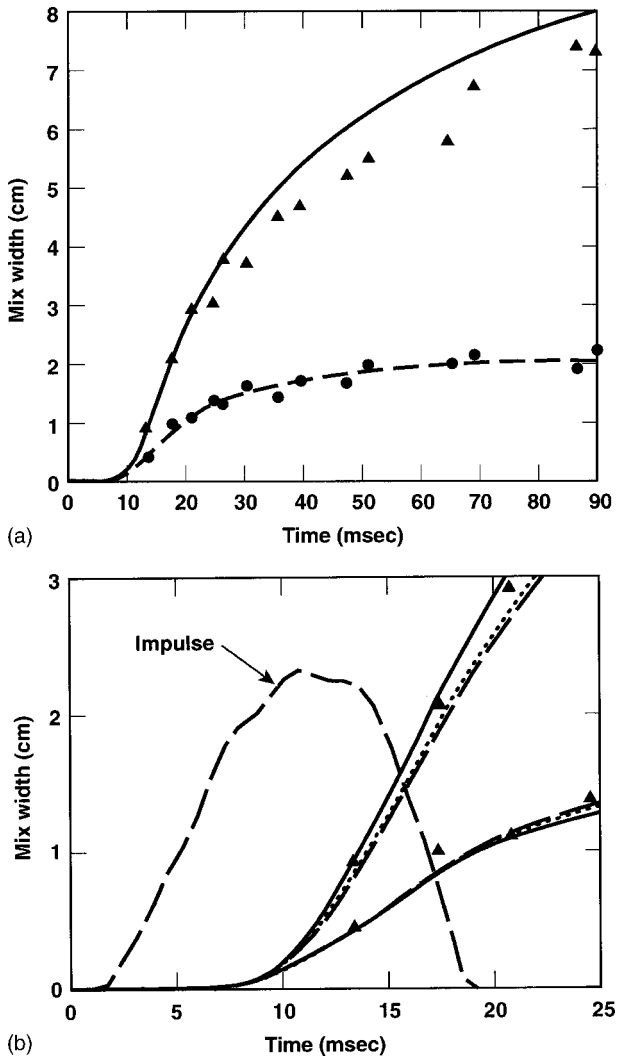

FIG. 1. (a) Time (ms) evolution of the thickness of the turbulent mixing zone (cm). Results of the LEM measurement are shown in triangles (spikes) and circles (bubbles). Results from our model calculation are shown in solid and dashed lines, respectively. (b) The early time evolution of the mixing zone amplitude and the impulse acceleration of the LEM experiment. The early time evolution of the amplitude is used to calibrate the drag coefficient and to pick the initial amplitude [the curves show the different attempts that lead to the result reported in (a)].

fully designed physical experiments [12,13]. We now collect all the model constants for the K-ε turbulence models,

$$C_\mu = 0.09, \quad \sigma_K = 0.87, \quad \sigma_\varepsilon = 1.30, \quad \sigma_i = .90,$$

$$C_{\varepsilon 1} = 1.44, \text{ and } C_{\varepsilon 2} = 1.92.$$

IV. COMPARISON AGAINST RTI AND RMI EXPERIMENTS

We will first compare our model against a turbulent Rayleigh-Taylor instability experiment by Dimonte and Schneider [26]. The impulsive acceleration experiment was conducted using a linear electric motor (LEM) with incompressible immiscible fluids. The density ratio between the heavy and light fluid is 23.4, which leads to 0.92 Atwood number. The light fluid is pressurized SF_6 gas and the heavy fluid is a hydrocarbon (Freon) because the surface tensions are low. In Fig. 1(a) we illustrate that the model calculations can produce good agreements with experimental data on the mixing fronts for the penetrations of the bubbles and spikes. The shape of the impulse and the early growth of the amplitude are illustrated in Fig. 1(b). The initial wavelength is estimated based on the values measured in the experiment. The initial amplitude and the drag coefficient (2.5) are cho-

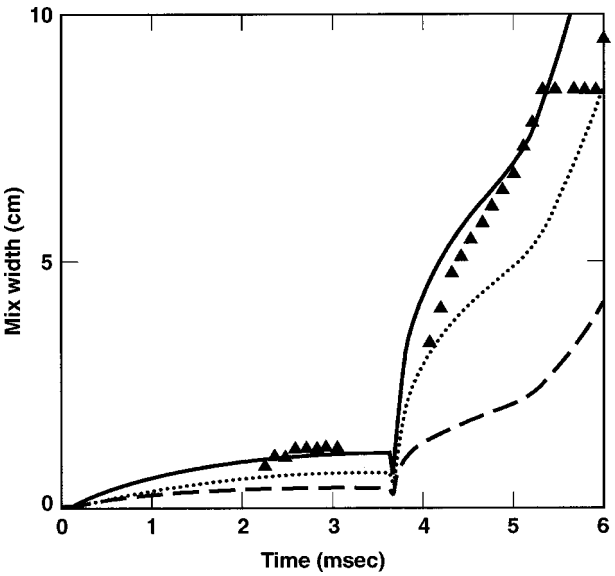

FIG. 2. Time evolution (ms) of the thickness of the turbulent mixing zone (mm). The result from the shock-tube measurement is illustrated by triangles. The model calculation is shown by solid line. Also shown are the model calculations of the bubble (dashed line) and spike (dotted line) amplitudes

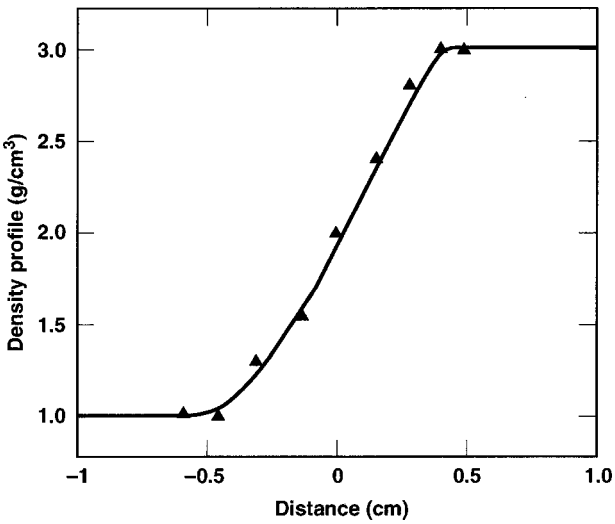

FIG. 3. The distribution of the average density profile in the mixing zone. Results of the constant acceleration experiment by Kucherenko *et al.* are shown by triangles. The model calculation is in shown by solid line.

sen to fit the initial growth of the mixing width envelope measured by the LEM experiment. Also shown in Fig. 1(b) are several curves from which we studied the sensitivity of the model to the different model parameters, such as the drag coefficient and initial amplitude.

We also compare our model calculation against a Richtmyer-Meshkov instability experiment conducted by Vetter and Sturtevant [27]. The experiment was performed in the 17-inch-diameter horizontal shock tube with an impulsively accelerated plane interface between air and SF_6. The shock tube used had a larger test section than in previous experiments so that the influence of the shock wave/boundary-layer interactions is no longer dominant. The Mach number is 1.5. Again, we demonstrate in Fig. 2 that our model calculation is in good agreement with experimental data. Note that in this experiment, there is a reshock. The model has a shock detection mechanism based on the ratio Q/P. The velocity difference is obtained by integrating over the zones and the resulting value is employed in the source term of the buoyancy-drag model at the end of shock passage.

Finally, we turn our attention to inspect the performance of our model against a constant acceleration experiment conducted by Kucherenko *et al.* [28]. Accurate data were obtained from the facilities (EKAP and SOM—complex test benches to study turbulent mixing with application of pulse x-ray methods, and pulse light methods, respectively) located at the All-Union Research Institute of Technical Physics, Chelyabinsk, Russia. Special care with experimental conditions was taken to ensure that the possible deviations from the self-similar mode of mixing are minimized. Indeed, the late time solution of our model reproduced the $h_i = \alpha A g t^2$ behavior. In Fig. 3, we compare our model calculation against the experiments regarding the distribution of the average density in the mixing zone. The Atwood number is 0.5. Again, our model has shown excellent agreement with experimental results.

V. SUMMARY

In summary, we have developed a two-scale transport model for the turbulent mix induced by the Rayleigh-Taylor and Richtmyer-Meshkov instabilities. We generalize the buoyancy-drag model by adding an energy equation for a more complete description of the generated interpenetration between the heavy and light fluids. The generalized buoyancy-drag model provides an appropriate source to the two-equation turbulence model. The two-scale transport model has shown to agree well with the impulsive acceleration experiment from the linear electric motor (LEM) [26] the Richtmyer-Meshkov experiment data from the Mach number 1.5 shock tube at Caltech [27], and finally, the constant acceleration Rayleigh-Taylor experiment at the All Union Research Institute of Technical Physics, Russia [28].

ACKNOWLEDGMENTS

This work was performed under the auspices of the U.S. Department of Energy by the University of California, Lawrence Livermore National Laboratory under Contract No. W-7405-Eng-48.

[1] Lord Rayleigh, *Scientific Papers* (Cambridge University Press, Cambridge, 1900), Vols. 2, 200.
[2] G. I. Taylor, Proc. R. Soc. London, Ser. A **201**, 192 (1950).
[3] R. D. Richtmyer, Commun. Pure Appl. Math. **13**, 297 (1960).
[4] E. E. Meshkov, Soviet Fluid Dynamics **4**, 101 (1969).
[5] L. Smarr, J. R. Wilson, R. P. Barton, and R. L. Bowers, Astrophys. J. **246**, 515 (1981); W. D. Arnett, J. N. Bahcall, R. T. Kirshner, and S. E. Woosley, Annu. Rev. Astron. Astrophys. **27**, 629 (1989).
[6] J. Lindl, *Inertial Confinement Fusion: The Quest for Ignition and Energy Gain* (Springer, New York, 1997).
[7] D. Layzer, Astrophys. J. **122**, 1 (1955); R. Clift, J. R. Grace, and M. E. Weber, *Bubbles, Drops and Particles* (Academic, New York, 1978); M. J. Lighthill, *An Informal Introduction to Theoretical Fluid Mechanics* (Oxford University Press, Oxford, UK, 1986).
[8] J. C. Hanson, P. A. Rosen, T. J. Goldsack, K. Oades, P. Fieldhouse, N. Cowperthwaite, D. L. Youngs, N. Mawhinney, and A. J. Baxter, Laser Part. Beams **8**, 51 (1990).
[9] D. Shvarts, O. Sadot, D. Oron, A. Rikanati, and U. Alon, in *Handbook of Shock Waves*, edited by G. Ben-Dor, O. Igra, and T. Elperin (Academic, San Diego, 2000), Vol 2.
[10] G. Dimonte, Phys. Plasmas **7**, 2255 (2000).
[11] B. Cheng, J. Glimm, and D. H. Sharp, Phys. Lett. A **268**, 366 (2000).
[12] C. G. Speziale, Annu. Rev. Fluid Mech. **23**, 107 (1991).
[13] S. Gauthier and M. Bonnet, Phys. Fluids A **2**, 1685 (1990).
[14] G. L. Mellor and H. J. Herring, AIAA J. **11**, 590 (1973).
[15] Y. Zhou, Phys. Fluids **13**, 538 (2001).
[16] D. A. Drew and S. L. Passman, *Theory of Multicomponent Fluids* (Springer, New York, 1999).
[17] D. L. Youngs, Physica D **37**, 270 (1989).
[18] D. L. Youngs, Laser Part. Beams **12**, 725 (1994).
[19] B. E. Launder and D. B. Spalding, *Mathematical Models of Turbulence* (Academic, London, 1972).
[20] K. Hanjalić, B. E. Launder, and R. Schiestel, *Turbulent Shear Flows 2*, Selected Papers From the Second International Symposium on Turbulent Shear Flows, London, 1979 (Springer, Berlin, 1980).
[21] R. Schiestel, Phys. Fluids **30**, 772 (1987).
[22] C. G. Speziale, Proceedings Of the 20th Symposium on Naval Hydrodynamics, 1995 (unpublished).
[23] E. J. Caramana, M. J. Shashkov, and P. P. Whalen, J. Comput. Phys. **144**, 70 (1998).
[24] U. Alon and D. Shvarts, in *Proceedings of the Fifth International Workshop on Compressible Turbulence Mixing*, edited by R. Young, J. Glimm, and B. Boston (Cambridge University Press, Cambridge, 1996).
[25] B. Cheng, J. Glimm, and D. H. Sharp, Z. Angew. Math. Phys.

(to be published).
[26] G. Dimonte and M. Schneider, Phys. Fluids **12**, 304 (2000).
[27] M. Vetter and B. Sturtevant, Shock Waves **4**, 247 (1995).
[28] Yu. A. Kucherenko, L. I. Shibarshov, V. I. Chitaikin, S. I. Balabin, A. P. Pylaev, in *Proceedings of the Third International Work on the Physics of Compressible Turbulent Mixing, Abbey of Rayaumont, France, 1991* (World Scientific, Singapore, 1991).